Analytical Methods

Accepted Manuscript

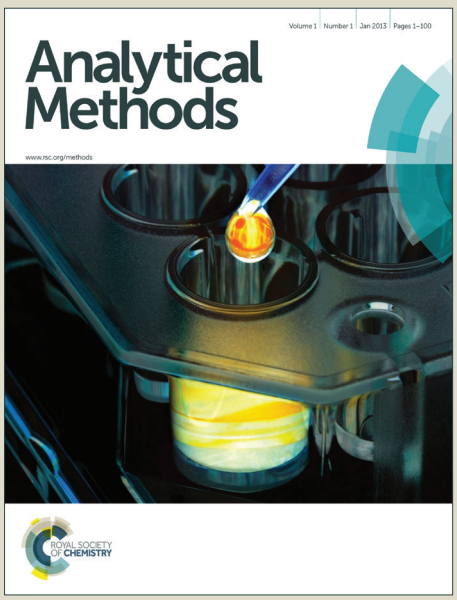

ROYAL SOCIETY OF CHEMISTRY

www.rsc.org/methods

TOC

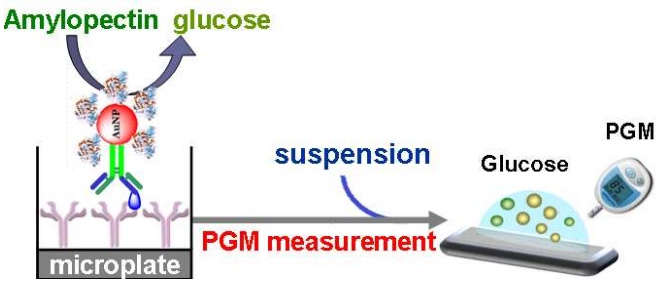

Cite this: DOI: 10.1039/c0xx00000x

www.rsc.org/xxxxxx

PAPER

A portable and quantitative enzyme immunoassay of neuron-specific enolase with gluometer readout

Xiaohong Fu,* Xueru Feng, Kun Xu and Rong Huang

Received (in XXX, XXX) Xth XXXXXXXXX 200X, Accepted Xth XXXXXXXXX 200X

DOI: 10.1039/b000000x

A portable and quantitative enzyme immunoassay with glucometer readout was developed for sensitive monitoring of neuron-specific enolase (NSE, as a model analyte) in a high-binding polystyrene 96-well microtiter plate (MTP), conjugated with monoclonal mouse anti-human NSE antibody (mAb_1). Gold nanoparticle heavily functionalized with glucoamylase and polyclonal rabbit anti-human NSE antibody (pAb_2) was utilized as the trace tag. A sandwich-type immunoassay format was adopted for quantitative detection of NSE in mAb_1-functionalized MTP. Accompanying the gold nanoparticle, the carried glucoamylase could hydrolyze amylopectin in glucose. The produced glucose could be quantitatively monitored using a portable personal glucose meter (PGM). Under optimal conditions, the PGM-based immunoassay exhibited good analytical properties for the determination of the target NSE, and allowed detection of NSE at concentrations as low as 0.05 ng mL^{-1}. Intra- and interassay coefficients of variation (CVs) were below 10% and 11%, respectively. The methodology was also evaluated by assaying 15 clinical serum samples, and showed good accordance between results obtained by the developed immunoassay and the referenced values.

Introduction

Enzyme immunoassay (EIA) and enzyme-linked immunosorbent assay (ELISA) are both widely used as diagnostic tools in medicine and as quality control measures in various industries.[1] EIA/ELISA uses the basic immunology concept of an antigen binding to its specific antibody, which allows determination of very small quantities of antigens such as proteins, peptides, hormones, or antibody in a fluid sample.[2] And more sophisticated analytical devices, such as surface plasmon resonance (SPR), quartz crystal microbalance (QCM), optical detection methods including fluorescence and chemiluminescence, and electrochemical method, have been studied on the basis of various signal generation principles from complex interaction between antibody and antigen.[3] Unfortunately, conventional methods usually require costly and complicated analytical instruments, as well as skilled personnel. Hence, recent research has been seeking to develop innovative and powerful detection schemes with the aim of manufacturing portable and affordable devices for the development of advanced immunoassays.

Glucose meter (or glucometer) is a medical device for determining the approximate concentration of glucose in the blood.[4] The device is among the few widely available and affordable tool that can provide quantitative measurement.[5] Recent researchers have combined simple, portable and inexpensive glucose meters with molecular sensors to measure a number of target molecules in blood, serum, water or food. For example, Xiang and Lu demonstrated the method to use such meters to quantify non-glucose targets, ranging from a recreational drug (cocaine) to an important biological cofactor (adenosine), to a disease marker (interferon-gamma of tuberculosis) and a toxic metal ion (uranium).[6] The method was based on target-induced release of invertase from a functional-DNA-invertase conjugate, and the released invertase converted sucrose into glucose. Xu et al. also constructed a convenient and highly sensitive sandwich approach for the detection of HIV DNA fragments that employed the easily accessible glucometer as the signal transducer.[7] Su et al. reported a new sensing strategy for sensitive and selective detection of copper ion based on multi-invertase conjugated magnetic bead signal amplification labels and a glucometer transducer by coupling with click chemistry.[8] Most recently, Yan and co-worker combined a glucoamylase-trapped aptamer-cross- linked hydrogel with a PGM for portable and quantitative detection of non-glucose targets.[9] Inspired by these strategies, our motivation in this work is to utilize the portable and quantitative glucometer for the development of advanced immunoassay by coupling with conditional enzyme immunoassay format.

Neuron-specific enolase (NSE) is a substance that has been detected in patients with certain tumors, namely neuroblastoma, small cell lung cancer, medullary thyroid cancer, carcinoid tumors, pancreatic endocrine tumors, and melanoma.[10] Herein, we used NSE as a model analyte to construct a glucometer-based enzyme immunoassay. Initially, monoclonal mouse anti-human NSE antibody (mAb_1) was immobilized into a high-binding polystyrene 96-well microtiter plate (MTP), and then gold nanoparticle with 16 nm in diameter heavily functionalized with glucoamylase and polyclonal rabbit anti-human NSE antibody

(pAb_2) was used as the detection antibody. In the presence of target NES, a sandwiched immunocomplex was formed in the MTP by using functional gold nanoparticle as the trace tag. The carried glucoamylase followed by gold nanoparticle could hydrolyze the amylopectin into multiple glucose molecules. The produced glucose molecules could be determined by using an external glucometer. By monitoring the signal of the glucometer, we could quantitatively judge the concentration of target NSE in the sample.

Experimental

Materials and reagent

Polyclonal rabbit anti-human NSE antibody (pAb), monoclonal mouse anti-human NSE antibody (mAb) and NSE standards with various concentrations were purchased from Beijing Biosynth. Biotechnol. Co., Ltd. (Beijing, China). Glucoamylase from *Aspergillus niger* (140 000 units mL^{-1}, solution) was obtained from Wuxi Syder Bio-products Co., Ltd (China). Amylopectin from potato starch and bovine serum albumin (BSA) were purchased from Sigma-Aldrich. All other reagents were of analytical grade and were used without further purification. Ultrapure water obtained from a Millipore water purification system (≥18 MΩ, Milli-Q, Millipore) was used in all runs. Personal glucose meter (PGM) buffer (pH 7.3) was consisted of 72.9 mM Na_2HPO_4, 27.1 mM NaH_2PO_4, 50 mM NaCl and 5 mM $MgCl_2$.

A pH 9.6 coating buffer (1.59 g Na_2CO_3, 2.93 g $NaHCO_3$ and 0.2 g NaN_3) and a pH 7.4 phosphate-buffered saline (PBS, 0.01 M) (2.9 g $Na_2HPO_4 \cdot 12H_2O$, 0.24 g KH_2PO_4, 0.2 g KCl and 8.0 g NaCl) were prepared by adding the corresponding chemicals into 1000 mL distilled water, respectively. The blocking buffer and washing buffer were obtained by adding 1.0% BSA (w/v) and 0.05% Tween 20 (v/v) in PBS, respectively.

Preparation of gold colloids

Gold colloids with 16 nm in diameter were prepared according to the literature.[11] All glassware used in the following procedures was cleaned in a bath of freshly prepared solution (3 : 1, $K_2Cr_2O_7$-H_2SO_4), thoroughly rinsed with double distilled water, and dried prior to use. Colloidal gold was prepared by adding 2.5 mL of 1.0 wt % sodium citrate solution into 100 mL of 0.01 wt % $HAuCl_4$ boiling solution. The maximum adsorption of the as-synthesized colloidal gold in UV-vis absorption spectroscopy was at 518 nm and the solution was stored in a refrigerator with a dark-colored glass bottle before use.

Preparation of glucoamylase/pAb_2-conjugated colloidal gold (GA-AuNP-pAb_2)

The GA-AuNP-pAb_2 conjugates were synthesized and prepared according to the literature.[3a] Prior to synthesis, 5 mL of 16-nm gold colloids (AuNP, $C_{[Au]}$ = 24 nM) was initially adjusted to pH 9.0-9.5 by directly using 0.1 M Na_2CO_3 aqueous solution. Then, 150 μL of 140 000 units mL^{-1} glucoamylase and 10 μL of 1.0 mg mL^{-1} pAb_2 were added into gold colloids. After gentle shaking on the shaker for 1 h at room temperature, 110 μL of 1.0 wt % polyethylene glycol was injected, and the mixture was transferred to the refrigerator at 4 °C for further reaction (overnight). Following that, the resultant mixture was repeatedly centrifuged at 4 °C for 20 min (14 000 g). The obtained pellet (i.e. GA-AuNP-pAb_2) was re-suspended in 0.5 mL of 2 mM sodium carbonate solution containing 1.0 wt % BSA and 0.1 wt % sodium azide, pH 7.4, and stored at 4 °C until use.

Immunoassay protocol and PGM measurement procedure

Scheme 1 displays the measurement process of PGM-based immunoassay. A high-binding polystyrene 96-well microtiter plates (Ref. 655061, Greiner, Frickenhausen, Germany) were coated overnight at 4 °C with 50 μL per well of mAb_1 at a concentration of 10 μg mL^{-1} in 0.05 M sodium carbonate buffer (pH 9.6). The microplates were covered with adhesive plastics plate sealing film to prevent evaporation. On the following day, the plates were washed three time with the washing buffer, and then incubated with 300 μL per well of blocking buffer for 1 h at 37 °C with shaking. The plates were then washed as before. Following that, 50 μL of NSE standards or samples with various concentrations in pH 7.4 PBS were added into the microtiter plates, and incubated for 1 h at 37 °C under shaking. After washing, 50 μL of the prepared-above GA-AuNP-pAb_2 suspension was added into the well and incubated for 1 h at 37 °C with shaking. The plates were washed again, and 20 μL of 0.5 mg mL^{-1} amylopectin in PGM buffer was added to each well. The plates were shaken for 40 min at 50 ºC on a plate shaker for hydrolysis of amylopectin. Following that, a 3-μL aliquot of the supernatant was removed for glucose measurement by using a commercialized Sannuo PGM (Sinocare Inc. Changsha, P.R. China, ≤ 27.8 mM). The obtained PGM signal was registered as the immunosensing signal relative to different-concentration target analytes. All measurements were carried out at room temperature (25 ± 1.0 ºC). All data were obtained with three measurements each in parallel.

Statistical analysis

All measurements were carried out in triplicate. All current responses recorded in this study were subtracted from the corresponding primary current as the baseline unless specified otherwise. A statistical data analysis was performed using SAS ver. 9.0 and SPSS ver. 9.0 softwares. Comparisons between dependent variables were determined using analysis of variance (ANOVA), Duncan multiple range test, correlation analysis and multiple regression analysis. Results were expressed as mean value ± standard deviation (SD) of three determinations and statistical significance was defined at $P \leq 0.05$.

Results and discussion

Principle and characterization of PGM-based immunoassay

In this work, the high-binding polystyrene 96-well microtiter plate is used for the immobilization of monoclonal mouse anti-human mAb_1 antibody based on the interaction between polystyrene and protein. The immobilization method is extensively employed in the commercialized ELISA.[12] Gold nanoparticles (16 nm) heavily functionalized with the glucoamylase and polyclonal rabbit anti-human pAb_2 antibody is utilized as the detection antibody. The association of glucoamylase and pAb_2 detection antibody to the colloidal

surface was possibly due to the interaction between cystein or NH_3^+-lysine residures of protein and gold nanoparticles.[13] The GA-AuNP-PAb_2 was qualitatively characterized using UV-vis absorption spectroscopy. As shown in Fig. 1a, the spectrum of bare AuNP exhibited a characteristic plasmon absorption peak at 517 nm. After the interaction between AuNP and glucoamylase/pAb_2, the plasmon absorption peak shifted from 517 nm to 522 nm, indicating the formation of bioconjugates.[14] This result could be also explained by using dynamic laser scattering (DLS). As shown from Fig. 1b, mixture of glucoamylase, pAb_2 and AuNP could result in the formation of the larger-sized nanocomposite (~21.6 nm) in comparison with AuNP alone (16.3 nm). Fig. 1c and 1d display typical TEM images of the as-synthesized AuNP and GA-AuNP-pAb_2, respectively. As seen from Fig. 1d, the size of GA-AuNP-pAb_2 was obviously larger than that of AuNP alone. Moreover, a layer of nanoshell on the surface of AuNP could be seemingly observed. Therefore, the GA-AuNP-pAb_2 could be successfully synthesized by using our designed route.

In a typical target NSE detection experiment, the immobilized mAb_1 in the MTP and the labeled pAb_2 on the AuNP sandwiched the target NSE, generating a complex with a large ratio of the glucoamylase and target NSE. When one antibody on the AuNP reacted with target antigen, other glucoamylase molecules labeled on the AuNP would be carried over, and thus participate in the hydrolysis reaction. Relative to antibody-enzyme conjugating protocol alone, the designed GA-AuNP-pAb_2 would exhibit higher catalytic efficiency toward amylopectin. Upon addition of amylopectin, the carried glucoamylase accompanying the AuNP could hydrolyze the amylopectin in multiple glucose molecules. The generated glucose molecules in the resulting solution were collected and detected by using an external PGM. By monitoring the change in the PGM signal, we can indirectly determine the level of target NSE. With the increasing target NSE, the PGM signal increases with the increment of target NSE in the sample. The PGM-based sensing platform for the detection of NSE is schematically illustrated in Scheme 1.

Optimization of experimental conditions

To acquire an optimal analytical performance, some experimental conditions including the hydrolysis time of amylopectin by the glucoamylase and the incubation time for the hydrolysis reaction should be optimized. Typically, the PGM signal derives from the generated glucose molecules by the hydrolysis reaction. Fig. 2a shows the effect of various hydrolysis times on the PGM signal by using 5 ng mL^{-1} NSE as an example. As indicated from Fig. 2a, the PGM signal increased with the augmentation of hydrolysis time from 0 to 60 min, and tended to level off after 40 min. Longer time did not obviously change the output signals of PGM, indicating that the hydrolysis reaction bascially tended to the equilibrium. Therefore, 40 min was used as the hydrolysis reaction time for the amylopectin.

Usually, the temperature directly affected the ratio of the hydrolysis reaction. Fig. 2b represents the temperature-dependent signal changes upon hydrolysis reaction of the amylopectin. As seen from Fig. 2b, the optimal PGM signal was obtained at 50 ºC. The reason might be most likely a consequence of the fact that the glucoamylase exhibited low hydrolysis capacity at the low temperature, while the bioactivity of the glucoamylase was hindered at the high temperature. As seen from the official homepage of glucoamylase producer (http://www.syder.com/EnProductShow.asp?ID=11), the effective temperature of the glucoamylase was 40 – 65 ºC. Considering the issue, 50 ºC was used for the progression of the hydrolytic reaction in this work.

Control test

Logically, a puzzled question to be produced is whether the PGM signal derived from the non-specific absorption of GA-AuNP-pAb_2 and the added amylopectin. To clarify this point, several control tests toward mAb_1-functionalized microtiter plate were carried out by the incubation of the following analytes: (i) GA-AuNP-pAb_2, (ii) amylopectin, (iii) GA-AuNP-pAb_2 + amylopectin, (iv) 5 ng mL^{-1} NSE + GA-AuNP-pAb_2, (v) 5 ng mL^{-1} NSE + amylopectin, and (vi) 5 ng mL^{-1} NSE + GA-AuNP-pAb_2 + amylopectin (5 ng mL^{-1} NSE used as an example). As seen from Columns '*d-f*' in Fig. 3, the PGM signal derived from the labeled glucoamylase toward the hydrolysis of amylopectin in the presence of target NSE (Column '*f*'). Moreover, GA-AuNP-pAb_2 (Column '*a*') and amylopectin (Column '*b*') could not cause the generation in the PGM signal. At the absence of target NSE, GA-AuNP-pAb_2 could not non-specifically adsorb onto the mAb_1-functionalized microtiter plate, thereby could not result in the shift of PGM signal regardless of the presence of amylopectin (Column '*c*'). Thus, the non-specific absorption of the PGM-based immunoassay should be ignored during the PGM measurement.

Calibration plots for PGM-based immunoassay towared NSE standards

Next, the PGM-based immunoassay was applied for quantifying NSE standards with various concentrations by using the as-synthesized GA-AuNP-pAb_2 as the detection antibody in the mAb_1-functionalized microtiter plate. Reaction was implemented by the carried glucoamylase toward the hydrolysis of the added amylopectin. The produced glucose was measured by using an external PGM. Target NSE concentrations of 0 – 80 ng mL^{-1} were assayed with three measurements each in parallel. As seen from Fig. 4, samples containing NSE analyte were ability to produce the PGM signals, confirming that the developed immunoassay could response toward target NSE to induce the generation of glucose for the PGM readout. More importantly, the PGM signal was proportional to the concentration of NSE up to ~ 45 ng mL^{-1}, establishing the quantitative detection capability of the PGM-based immunoassay. The linear regression equation was y (mM) = $0.5044x + 2.1185$ (ng mL^{-1}, $R^2 = 0.9984$, $n = 30$). A limit of detection (LOD) with 0.05 ng mL^{-1} NSE was observed at the $3s_{Blank}$ criterion. Although our designed system has not yet been optimized for maximum efficiency, the LOD was partial lower than that of commercially available human NSE ELISA kits from CusaBio Biotech. Inc. (0.39 ng mL^{-1}), MyBioSource, Inc. (0.39 ng mL^{-1}, Cat# MBS704796, USA), Wuhan EIAab Sci. Co., Ltd (0.156 ng mL^{-1}, Cat# E0537h, China), Diagnostic Automation, Inc. (15 ng mL^{-1}, Cat# 6334Z, USA), USCN Life Sci. Inc. (0.0072 ng mL^{-1}, Cat# E90537Hu, USA), and Alpha Diagnostic Intl. (1.0 ng mL^{-1}, Cat# 0050, USA).

Specific, precision and reproducibility

The specificity of the PGM-based immunoassay was monitored by chanllenging the system against other biomolecules or

glycoproteins, such as squamous cell carcinoma antigen (SCCA, 50 ng mL^{-1}), myc-oncogene (MYC, 50 ng mL^{-1}), thyroid-stimulating hormone (TSH, 50 ng mL^{-1}), and alpha-fetoprotein (AFP, 50 ng mL^{-1}). As shown from Fig. 4a, these interferring agents did not cause the change in the PGM signal relative to blank serum sample, and the presence of only target NSE resulted in the obvious change in the signal. More importantly, the co-existance of interferring agents with target NSE exhibited the low shift in the PGM signal (RSD < 7.2%). The results indicated that the PGM-based immunoassay could be used for specific detection of target NSE.

The reproducibility and precision of the PGM-based immunoassay was also studied by repeatedly assaying three NSE standards with various concentrations, using identical batched of GA-AuNP-pAb_2 throughout. As seen from Table 1, the coefficients of variation (CVs) of the intra-assay between 5 runs were 9.8%, 7.1% and 5.3% for 0.5, 5, and 40 ng mL^{-1} NSE, respectively, whereas the CVs of the inter-assay with various batches were 10.8%, 9.5% and 8.9% towards the mentioned-above targets. The low CVs indicated the possibility of the PGM-based immunoassay with batch-wise preparation

Evaluation of method accuracy with real samples

To investigate the possible application of the PGM-based immunoassay for testing real human serum samples, we collected 3 clinical serum specimens containing target NSE from The Second People's Hospital of Sichuan Province. Initially, the specimens were diluted to 15 samples with various concentrations by using new-born cattle serum, and then these samples were assayed by using the PGM-based immunoassay. The obtained results were compared with the reference values obtained from the Electrochemiluminescent (ECL) Automatic Analyzer (provided by hospital) (Fig. 5b). Comparison of the experimental results between two methods was also performed *via* the use of a least-squares regression method. The regression line was $y = 0.9605x + 0.6976$ ($R^2 = 0.9923$, $n = 45$) (where x stands for NSE level estimated with the PGM-based immunoassay and y stands for the referenced values with the ECL-based immunoassay). The slope and intercept of the regression equation were close to ideal values '1' and '0', respectively. Thus, the developed PGM-based immunoassay could be preliminarily considered as an optional scheme for quantitative detection of target NSE in real samples.

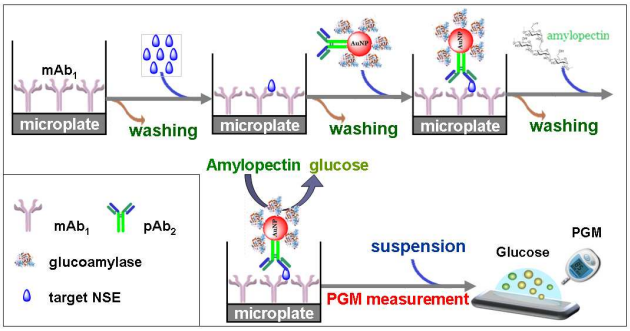

Scheme 1 Schematic illustration of the PGM-based immunoassay based on the hydrolysis reaction of the labeled glucoamylase toward the amylopectin.

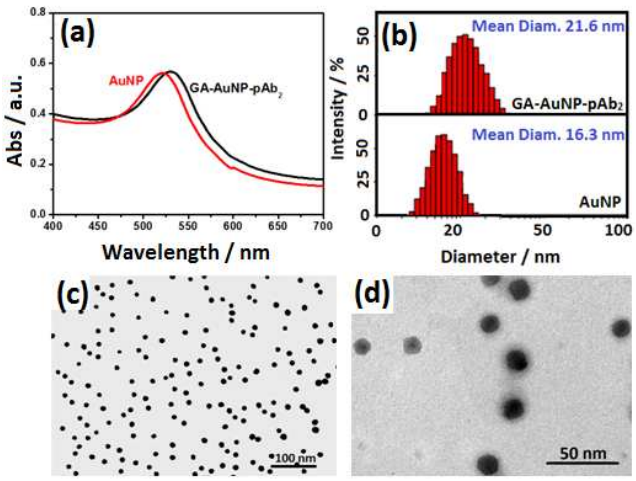

Fig. 1 (a) UV-vis absorption spectra of gold colloids and GA-AuNP-pAb_2, (b) DLS data of AuNP and GA-AuNP-pAb_2, and TEM image of (c) the as-synthesized AuNP and (d) GA-AuNP-pAb_2.

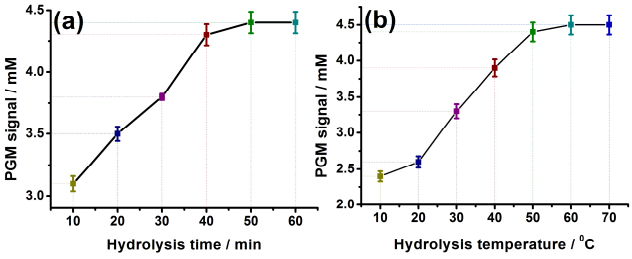

Fig. 2 The effect of (a) hydrolysis time and (b) hydrolysis temperature on the PGM signal of the developed immunoassay (5 ng mL^{-1} NSE used in this case).

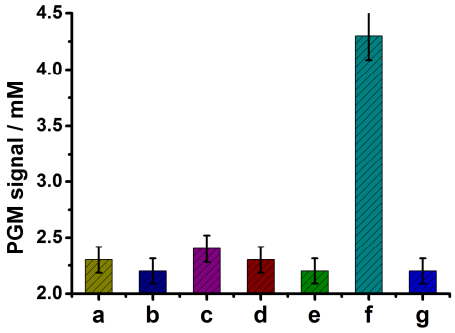

Fig. 3 PGM responses of the mAb_1-functionalized MTP toward various substrates: (a) GA-AuNP-pAb_2, (b) amylopectin, (c) GA-AuNP-pAb_2 + amylopectin, (d) 5 ng mL^{-1} NSE + GA-AuNP-pAb_2, (e) 5 ng mL^{-1} NSE + amylopectin, (f) 5 ng mL^{-1} NSE + GA-AuNP-pAb_2 + amylopectin, and (g) blank PGM buffer.

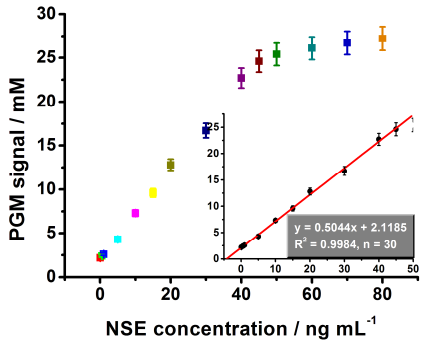

Fig. 4 Calibration curve for the PGM-based immunoassay using a range of standard NSE concentrations. Each data point represents the average value obtained from three different measurements. The error bars represent the 95% confidence interval of the mean for he PGM signal.

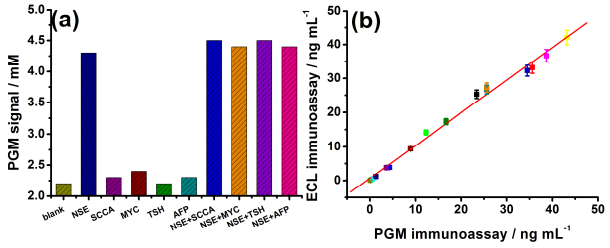

Fig. 5 (a) The specificity of the PGM-based immunoassay toward NSE, SCCA, MYC, TSH and AFP (5 ng mL^{-1} NSE used in this case), and (b) comparison of the assay results toward clinical serum samples by using the PGM-based immunoassay and the referenced ECL immunoassay method.

Conclusions

In summary, we report the proof-of-concept of new enzyme immunoassay for the detection of low-abundance protein (NSE used in this case) by coupling with a commercialized polystyrene microtiter plate and a portable personal glucose meter. Although the detection limit of the PGM-based immunoassay was relatively high, the developed method is more accessible for public use, especially in major developing countries, compared with standard instrumental sensing protocols. More importantly, the assay does not require sophisticated equipment and sample pretreatment, thus representing a versatile detection method.

Support by the Scientific Research Fund of Sichuan Provincial Education Department (grant nos. 11ZA231 & 14ZA0303), the Natural Science Foundation of Sichuan Province, and the Key Project of Chengdu Normal University (grant no. CS13ZA02) is gratefully acknowledged.

Table 1 Precision and reproducibility (coefficient of variation, CV) of determinations using identical batches of GA-AuNP-pAb_2 throughout

Item	$C_{[NSE]}$, ng mL^{-1}	Identical batches;[a] Assay concentration (ng mL^{-1})					CV (%,)
		1	2	3	4	5	
Intra-assay	0.5	0.47	0.54	0.51	0.47	0.59	9.8
	5	5.4	5.2	4.8	4.9	5.7	7.1
	40	37.8	43.2	41.2	39.3	38.9	5.3
Inter-assay	0.5	0.47	0.52	0.59	0.45	0.54	10.8
	5	5.9	4.6	5.4	4.9	5.2	9.5
	40	43.6	37.8	46.2	37.8	41.3	8.9

[a] The CVs (n = 5) of intra-assay were obtained by using the same-batch GA-AuNP-pAb_2, whereas the CVs of the inter-assay were achieved by using various batches.

Notes and references

Department of Chemistry and Applied Chemistry, Chengdu Normal University, Chengdu 611130, P.R. China. E-mail: xiaohong.fuzq@gmail.com; Fax: +86 28 6677 2014; Tel: +86 28 6677 2040

1 (*a*) S. Gan and K. Patel, *J. Invest. Dermatol.*, 2013, **133**, e12; (*b*) R. Castro, E. Prieto, I. Santo, J. Azevedo, and F. Exposto, *J. Clin. Microbiol.*, 2013, **41**, 250-253.

2 (*a*) E. Dobrovolskaia, A. Gam, and J. Slater, *Clin. Exp. Allergy*, 2006, **36**, 525-530; (*b*) P. Connolly, C. Hage, J. Bariola, E. Bensadoun, M. Rodgers, R. Bradsher Jr, and L. Wheat, *Clin. Vaccine Immunol.*, 2012, **19**, 53-56.

3 (*a*) D. Tang, B. Zhang, J. Tang, L. Hou, and G. Chen, *Anal. Chem.*, 2013, **85**, 6958-6966; (*b*) D. Tang, B. Su, J. Tang, J. Ren, and G. Chen, *Anal. Chem.*, 2010, **82**, 1527-1534; (*c*) J. Homolar, S. Yee, and G. Gauglitz, *Sens. Auctu. B*, 1999, **54**, 3-15; (*d*) Y. Wang, L. Tang, J. Jiang, *Anal. Chem.*, 2013, **85**, 9213-9220; (*e*) T. Konz, E. Alvarez, M. Montes-Bayon, and A. Sanz-Medel, *Anal. Chem.*, 2013, **85**, 8334-8340.

4 (*a*) M. Amer, *J. Med. Engin. Technol.*, 2002, **26**, 208-213; (*b*) L. Rao, F. Jakubiak, J. Sidwell, J. Winkelman, and M. Snyder, *Clin. Chim. Acta*, 2005, **356**, 178-183; (c) H. Mohapatra and S. Phillips, *Chem. Commun.*, 2013, **49**, 6134-6136.

5 (*a*) P. Barreau and J. Buttery, *Diabetes Care*, 1988, **11**, 116-118; (*b*) B. Harrison, R. Markes, P. Bradley, and I. Ismail, *Clin. Biochem.*, 1996, **29**, 521-527.

6. (*a*) Y. Xiang and Y. Lu, *Nat. Chem.*, 2011, **3**, 697-703; (*b*) Y. Xiang and Y. Lu, *Anal. Chem.*, 2012, **84**, 4174-4178; (c) Y. Xiang and Y. Lu, *Anal. Chem.*, 2012, *84*, 1975-1980; (*d*) Y. Xiang and Y. Lu, *Chem. Commun.*, 2013, **49**, 585-587; (e) J. Su, J. Xu, Y. Chen, Y. Xiang, R. Yuan and Y. Chai, *Chem. Commun.*, 2012, **48**, 6909-6911.

7 J. Xu, B. Jiang, J. Xie, Y. Xiang, R. Yuan and Y. Chai, *Chem. Commun.*, 2012, **48**, 10733-10735.

8 J. Su, J. Xu, Y. Chen, Y. Xiang, R. Yuan and Y. Chai, *Biosens. Bioelectron.*, 2013, **45**, 219-222.

9 L. Yan, Z. Zhu, Y. Zou, Y. Huang, D. Liu, S. Jia, D. Xu, M. Xu, Y. Zhou, S. Zhou, and C. Yang, *J. Am. Chem. Soc.*, 2013, **135**, 3748-3751.

10 (*a*) R. Dittadi and M. Gion, *Clin. Biochem.*, 2013, **46**, 1145-1145; (*b*) N. Tolan, N. Vidal-Folch, A. Algeciras-Schimnich, R. Singh, and S. Grebe, *Clin. Chim. Acta*, 2013, **424**, 216-221.

11 B. Zhang, B. Liu, D. Tang, R. Niessner, G. Chen, and D. Knopp, *Anal. Chem.*, 2012, **84**, 5392-5399.

12 (*a*) C. Cervino, E. Weber, D. Knopp, and R. Niessner, *J. Immunol. Method*, 2008, **329**, 184-193; (*b*) S. Parween and P. Nahar, *Biosens. Bioelectron.*, 2013, **48**, 287-292; (*c*) C. Marquette, B. Corgier, and L. Blum, *Bioanalysis*, 2012, **4**, 927-936.

13 G. Hermanson, *Bioconjugate Techniques*, 2nd ed., Academic Press, San Diego, 2008, p 925.

14 (*a*) Z. Gao, M. Xu, L. Hou, G. Chen, and D. Tang, *Anal. Chem.*, 2013, **85**, 6945-6952; (*b*) J. Zheng, A. Jiao, R. Yang, H. Li, J. Li, M. Shi, C. Ma, Y. Jiang, L. Deng, and W. Tan, *J. Am. Chem. Soc.*, 2012, **134**, 19957-19960.